Extreme Low-Flow Conditions in a Dual-Chamber Denitrification Bioreactor Contribute to Pollution Swapping with Low Landscape-Scale Impact

Lindsey M. Hartfiel*[a], Natasha L. Hoover[b], Steven J. Hall[c], Thomas M. Isenhart[d], Carmen L. Gomes[e], Michelle L. Soupir[b]

[a] UW Discovery Farms, University of Wisconsin-Madison, Division of Extension, Madison, WI, United States
[b] Department of Agricultural and Biosystems Engineering, Iowa State University, Ames, IA, United States
[c] Department of Ecology, Evolution, and Organismal Biology, Iowa State University, Ames, IA, United States
[d] Department of Natural Resource Ecology and Management, Iowa State University, Ames, IA, United States
[e] Department of Mechanical Engineering, Iowa State University, Ames, IA, United States
*Corresponding author, email address: lindsey.hartfiel@wisc.edu

Abstract

Denitrification bioreactors are an effective edge-of-field conservation practice for nitrate (NO_3) reduction from subsurface drainage. However, these systems may produce other pollutants and greenhouse gases during NO_3 removal. Here a dual-chamber woodchip bioreactor system experiencing extreme low-flow conditions was monitored for its spatiotemporal NO_3 and total organic carbon dynamics in the drainage water. Near complete removal of NO_3 was observed in both bioreactor chambers in the first two years of monitoring (2019-2020) and in the third year of monitoring in chamber A, with significant (p<0.01) reduction of the NO_3-N each year in both chambers with 8.6–11.4 mg NO_3-N L^{-1} removed on average. Based on the NO_3 removal observed, spatial monitoring of sulfate (SO_4), dissolved methane (CH_4), and dissolved nitrous oxide (N_2O) gases was added in the third year of monitoring (2021). In 2021, chambers A and B had median hydraulic residence times (HRTs) of 64 h and 39 h, respectively, due to varying elevations of the chambers, with drought conditions making the differences more pronounced. In 2021, significant production of dissolved CH_4 was observed at rates of 0.54 g CH_4-C m^{-3} d^{-1} and 0.07 g CH_4-C m^{-3} d^{-1} in chambers A and B, respectively. In chamber A, significant removal (p<0.01) of SO_4 (0.23 g SO_4 m^{-3} d^{-1}) and dissolved N_2O (0.21 mg N_2O-N m^{-2} d^{-1}) were observed, whereas chamber B produced N_2O (0.36 mg N_2O-N m^{-2} d^{-1}). Considering the carbon dioxide equivalents (CO_2e) on an annual basis, chamber A had loads (~12,000 kg CO_2e ha^{-1} y^{-1}) greater

than comparable poorly drained agricultural soils; however, the landscape-scale impact was small (<1% change in CO_2e) when expressed over the drainage area treated by the bioreactor. Under low-flow conditions, pollution swapping in woodchip bioreactors can be reduced at HRTs <50 h and NO_3 concentrations >2 mg N L^{-1}.

Keywords: woodchip bioreactor, nitrate, subsurface drainage, water quality, greenhouse gases, sulfate

1. Introduction

Excess nutrient loading to surface waters contributes to the formation of hypoxic zones through eutrophication and is a global water quality concern with over 400 hypoxic zones identified worldwide (Diaz & Rosenberg, 2008). In Europe, the Nitrates Directive was introduced in 1991 to target water quality improvements specifically related to nitrate reductions from agricultural sources with strategies to improve nutrient management (European Union, 1991). In 2000, the Water Framework Directive was introduced with a more holistic goal of improving surface and ground waters to a good chemical and ecological status (E.U. Water Framework Directive, 2000). In the United States, the Mississippi River/Gulf of Mexico Watershed Nutrient Task Force developed the 2008 Gulf Hypoxia Action Plan to reduce the size of the seasonal hypoxic zone in the Gulf of Mexico (Mississippi River/Gulf of Mexico Watershed Nutrient Task Force, 2008). As part of this plan, the twelve states bordering the Mississippi and Ohio Rivers developed nutrient reduction strategies to reduce both point and nonpoint source pollution (Mississippi River/ Gulf of Mexico Task Force, 2020). For example, the Iowa Nutrient Reduction Strategy calls for a 45% reduction in both nitrogen (N) and phosphorus (P) with 41% of N and 29% of P reductions coming from nonpoint sources (Iowa Department of Agriculture and Land Stewardship, 2017).

In Iowa and the Midwestern United States, subsurface tile drainage is a major contributor of excess nitrate-nitrogen (NO_3-N) loading to the Gulf of Mexico from nonpoint sources with concentrations as high as 77 mg NO_3-N L^{-1} observed for tile drainage systems, with significant reductions in tile drainage N loads needed to meet water quality goals (Ikenberry et al., 2014; Schilling et al., 2012). One conservation practice used to remove nonpoint source NO_3 is denitrifying bioreactors. Denitrifying bioreactors are a lined trench filled with a carbon (C) source, typically woodchips, that intercepts subsurface tile drainage. The C source enables microbial denitrification to occur in an engineered environment, allowing for conversion of NO_3 to dinitrogen (N_2) gas (Cameron & Schipper, 2010; Christianson et al., 2010). Denitrifying bioreactors have been explored since the 1990s (Blowes et al., 1994) and have proven to be effective at reducing NO_3 loading to downstream surface waters (Addy et al., 2016; Christianson et al., 2021). Bioreactors have also proven quite versatile in their global applications. For example, bioreactors have been used for treating aquaculture systems and effluents, springs, groundwater desalination brine, hydroponic wastewater, drainage ditches, and dairy farm effluents (Christianson et al., 2017; Christianson et al., 2016; Díaz-García et al., 2021; Easton et al., 2019; Pulkkinen et al., 2021; Schipper et al., 2010; Warneke et al., 2011). In a review of denitrification bioreactors around the world, median and mean percent NO_3 reductions of 46% and 40±26% have been reported, respectively, with a median mass removal rate of 5.1 g NO_3-N m^{-3} d^{-1} (Christianson et al., 2021).

Standards for the design of bioreactors for treating subsurface tile drainage in the U.S. have been produced by the USDA-NRCS Conservation Practice Code 605 (NRCS, 2020). These bioreactors are designed based on the size and slope of the incoming subsurface tile drainage line, frequently without data to support the flow conditions experienced at the site. Therefore, the

bioreactor design is heavily dependent on the subsurface drainage system design and there is potential for bioreactors to be over or under-designed. What is referred to as over-designed bioreactors experience lower than anticipated flowrates and volume of tile drainage with prolonged hydraulic residence times (HRTs). Here, the authors define extreme low-flow conditions within bioreactor systems as those whose median flow conditions are <10% of the design flow capacity. This criterion is based on the extreme flow conditions defined by the EPA in load duration curve analysis with the $<10^{th}$ and $>90^{th}$ percentiles being referred to as extreme hydrologic conditions (Serrano et al., 2020; US EPA, 2007).

Concerns have been raised in the design and implementation of over-designed bioreactors in terms of their potential for pollution swapping (i.e., trading a water quality problem for another water quality or air quality problem), especially under low- or high-flow conditions (Christianson et al., 2012; Davis et al., 2019; Healy et al., 2015; Healy et al., 2011; Shih et al., 2011). Upon bioreactor start up, high concentrations of the labile C source can be leached out of the bioreactor (David et al., 2016; Hoover et al., 2016), which is of environmental concern as the leached C can potentially stimulate microbial activity, reducing dissolved oxygen levels in downstream waterbodies (Schmidt & Clark, 2012). Throughout the bioreactor life, additional pollution swapping concerns may persist. Under high-flow conditions where the HRT is reduced, incomplete denitrification can occur leading to the production of nitrous oxide (N_2O), a harmful greenhouse gas (GHG) (Davis et al., 2019). Under low-flow conditions, complete denitrification can occur, followed by sulfate (SO_4) reduction (Blowes et al., 1994), which has been linked to methylmercury production in freshwater systems (Gilmour et al., 1992; Gilmour et al., 2013). The relationship between SO_4 reduction and methylmercury production is moderately weak and nonlinear (Marvin-DiPasquale et al., 2009), but is of concern in aquatic environments due to

methylmercury's ability to bioaccumulate (Sams, 2007).Under low-flow conditions, there is also concern for methane (CH_4) production, another GHG (Davis et al., 2019). The production of N_2O and CH_4 or reduction of SO_4 is driven by the redox potential within the bioreactor with reduction of NO_3 to N_2O gas followed by further reduction of N_2O to N_2 gas being most energetically favorable for the microbes under anaerobic conditions; once NO_3 has been removed, reduction of SO_4 and production of CH_4 can occur as these are further down the redox ladder with less energy released to the microbes (Chapin et al., 2011; Voroney & Heck, 2015).

While the NO_3 removal by denitrification bioreactors has been well-studied, the potential for harmful byproducts or pollution swapping under low-flow conditions in field-scale bioreactors is less understood. This study serves to monitor and evaluate the potential for pollution swapping and its landscape-scale impact in an unintentionally overdesigned bioreactor that has low-flow conditions, which were enhanced by drought conditions. The study objectives were to (i) evaluate how NO_3 and total organic carbon (TOC) concentrations varied spatially and temporally within the bioreactor, (ii) evaluate how the reduction of NO_3 spatially within the bioreactor relates to pollution swapping in terms of dissolved GHG production or SO_4 reduction, (iii) evaluate bioreactor design standard recommendations through the assessment of multiple pollutants over a range of HRTs, and (iv) assess the landscape-scale impact of the denitrification bioreactor operation under low-flow conditions. This study can be used to guide denitrification bioreactor management globally to minimize the risk of pollution swapping, especially for bioreactors treating subsurface drainage. Similar studies could be conducted for bioreactors treating alternative nitrate laden waters (e.g., aquaculture or hydroponic effluents) to improve their management. This information can also be used to further the discussion of how to improve current bioreactor designs.

2. Materials and Methods

2.1 Site Description

This study was conducted at the Iowa State University (ISU) Uthe farm (41°55’19’’N, 93°45’25’’W). A dual-chamber bioreactor, essentially two bioreactors connected in parallel, was installed in summer 2018 (Fig. 1). This site was designed as such to meet the criteria set in the USDA-NRCS design standard to treat approximately 17% of the peak flow from a 35.6 cm in diameter main tile line draining an estimated 36.8 ha area (NRCS, 2015). The final design from the USDA-NRCS resulted in two bioreactor chambers, referred to as chamber A and chamber B, to accommodate the large design flowrate from the tile drainage system. Each chamber has dimensions of 36.6 m long, 10.4 m wide, and 1.1 m deep with a designed slope of 0.17% and a flowrate of approximately 10.5 L s^{-1} from the combined outflow. The bioreactor chambers were both lined with 4 mil plastic on the bottom and sides, filled with NRCS design standard approved mixed hardwood chips sourced from J. Pettiecord, Inc., Bondurant, IA (Sean McCoy, Iowa Department of Land Stewardship- Division of Soil Conservation, personal communication, March 24, 2020), and covered with a geotextile fabric before adding a soil cap with a designed average depth of 0.30 m.

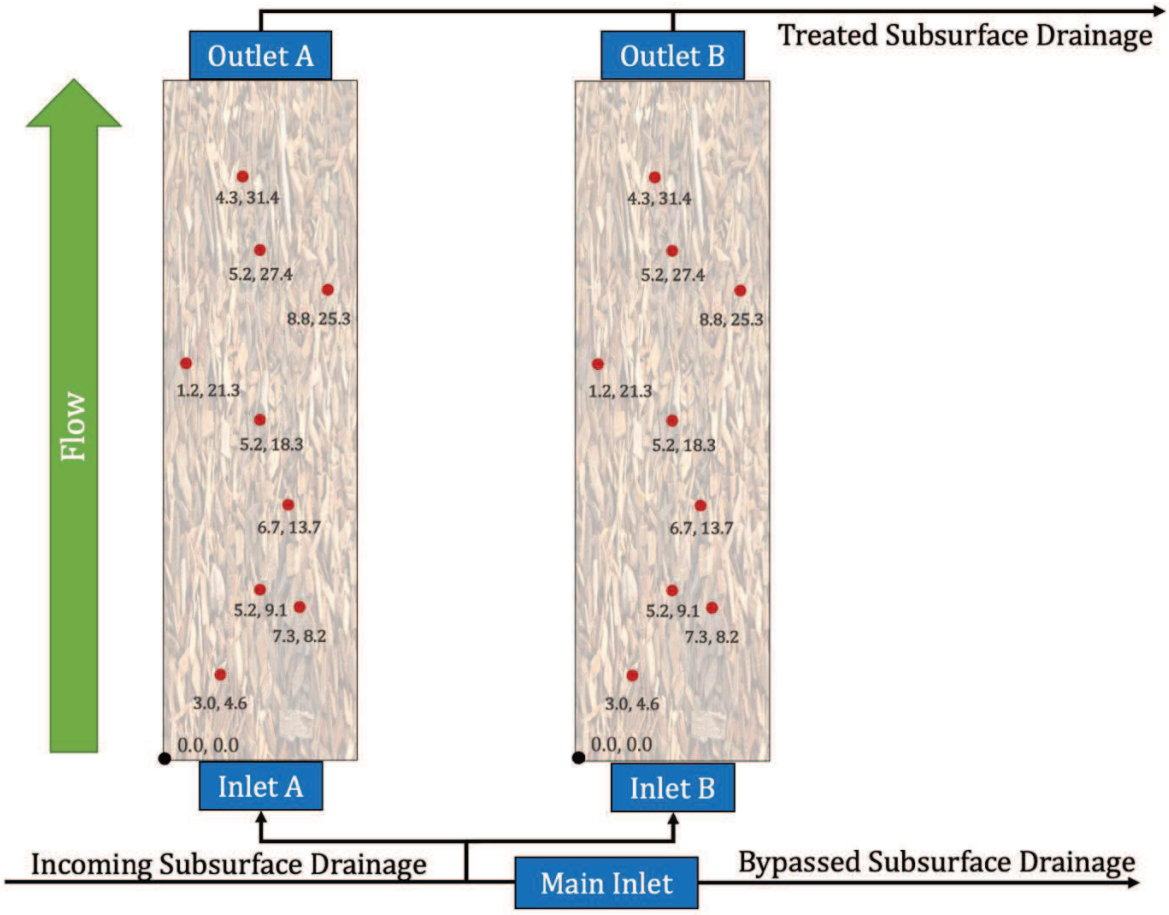

Figure 1. Bioreactor layout (top view) with sampling locations. Sampling wells are represented by red circles and their location with respect to bottom left corner of each chamber (black circles) are displayed as width (m), length (m). Water control structures are shown as blue rectangles. Lastly, the orientation of the incoming, treated, and by-passed subsurface drainage is shown. The treated and by-passed flow are released to a nearby creek.

As a dual-chamber bioreactor, the configuration of the water control structures at this site is unique compared to other bioreactor studies (Figure 1). The site features a main water control structure (Advanced Drainage Systems, Eagle Grove, IA), referred to as the main inlet, where the flow is directed into the two chambers or by-passed under high-flow conditions. Each bioreactor chamber also features a separate inlet and outlet water control structure (Advanced Drainage Systems, Eagle Grove, IA) equipped with a series of stacked PVC boards, referred to as stoplogs, that can be added or removed to adjust the water depth and set the corresponding hydraulic gradient. In the main inlet, a 61.0 cm wide V-Notch weir (Agri Drain Corporation, Adair, IA) is

used with a vented pressure transducer (Solinst Model 3250 LevelVent; Solinst, Ontario, Canada) to monitor by-passed flow. Each bioreactor chamber's outlet water control structure (referred to as outlet A and outlet B for chambers A and B, respectively) is configured similarly with a 30.5 cm wide V-Notch weir (Agri Drain Corporation, Adair, IA) and another vented pressure transducer (described in more detail in section 2.3). The by-passed and outlet flow drain to a nearby creek.

Before monitoring began in April 2019, flow entering the bioreactor was completely by-passed through the main inlet control structure. The two bioreactor chambers allow for replicate sampling as both chambers receive tile drainage from the same main tile line and experience the same ambient conditions (temperature and precipitation). Each bioreactor chamber includes nine sampling wells randomly located across both the length and width of the bioreactor (Fig. 1), allowing spatial sampling of NO_3 and other constituents. The sampling wells were constructed from 10.2 cm diameter PVC and range from 2.3 m to 2.6 m in height. The wells (Environmental Service Products, Irvine, CA) consist of slotted PVC (0.5 mm slot size) below the soil surface, allowing water to flow into the sampling well while keeping the bioreactor woodchips out. Above the surface of the bioreactor, the sampling wells were constructed of solid PVC. In April 2021, following two years of monitoring (2019 and 2020), an additional 40.6 cm main tile drainage line was added to the bioreactor inflow. This modification was approved by the Iowa USDA-NRCS following our initial monitoring.

2.2 Sample Collection

Initial sampling included NO_3-N and TOC at the main inlet and outlets A and B. Beginning in June of 2019, the sampling at this site was expanded to include collection of water quality samples from all sampling wells and water control structures. Samples from the wells were collected following the methods described in Table 1. Samples collected from the inlet and

179 outlet water control structures were collected in 1 L HDPE bottles using a sampling pole with the
180 bottle attached; submerging and rinsing the bottle, before submerging again to collect the
181 sample. Samples were stored on ice in the field and transported back to the Water Quality
182 Research Laboratory (WQRL) at ISU where they were stored at 4°C until analysis, following
183 preservation methods defined for the respective sample analysis methods (Table1). Frequency of
184 sample collection, details of the collection method, and preservation methods are summarized in
185 Table 1. Water samples were analyzed as NO_3-N + nitrite (NO_2-N) (Table 1) but were
186 interpreted as NO_3-N as this was the primary form of N present (Table S1). *In situ* measurements
187 of dissolved oxygen (YSI ProODO field probe), temperature (YSI ProODO field probe), and
188 water level (Solinst Water Level Meter Model 101; Solinst, Ontario, Canada) were taken from all
189 sampling locations.
190 Additional monitoring at this site began in 2021 after considering the 2019 and 2020
191 results. Samples for dissolved GHGs were collected from each water control structure and
192 sampling well following methods described in Table 1. Surface fluxes were not monitored as
193 previous work has demonstrated that dissolved fluxes are the predominant form in bioreactor
194 systems (Davis et al., 2019; Manca et al., 2021; Warneke et al., 2011). After transferring the
195 samples to evacuated vials and preserving with zinc chloride (Table 1), the vials were adjusted to
196 atmospheric pressure with helium. Prior to analysis, the vials were filled with an additional 7 mL
197 of helium and shaken for 30 minutes on a reciprocal shaker to equilibrate CH_4 and N_2O
198 concentrations with the headspace in the vial. Due to issues with equipment, the samples had to
199 be transferred from the 20 mL vials to a smaller, 12 mL Exetainer vial. To transfer the samples, 5
200 mL of the equilibrated headspace was collected from the 20 mL vial using a 20 mL syringe. The
201 5 mL sample was then injected into the evacuated 12 mL vial. Immediately, 15 mL of helium

was added to over-pressurize the vial and mix with the 5 mL sample. Also beginning in 2021, the 125 mL samples collected in the field were analyzed for SO_4 prior to acidifying the sample for later NO_3-N analysis.

Table 1. Summary of parameters monitored, frequency of monitoring, and methods of collection, analysis, and preservation.

	Water Quality Parameters				
	Nitrate-N (NO_3-N) + Nitrite-N (NO_2-N)	Sulfate (SO_4^{2-})	Total Organic Carbon (TOC)	Dissolved Methane (CH_4-C)	Dissolved Nitrous Oxide (N_2O-N)
Years Monitored	2019-2021	2021	2019-2021	2021	2021
Sampling Frequency	Weekly	Weekly	Monthly	Weekly	Weekly
Collection Method	Solinst peristaltic pump (Model 410; Solinst, Ontario, Canada) to fill 125 mL bottles purging wells for ~2.5 minutes prior to collection similar to Martin et al. (2019) and Davis et al. (2019); Subsampled from 1L bottle from water control structures		Subsampled (80 mL sample) from 125 mL sample bottles	Peristaltic pump to fill glass BOD bottle from wells. Subsampled 1L bottles immediately in field to fill glass BOD bottle from water control structures. In lab, transferred 10 mL duplicate samples to evacuated 20 mL vials	
Analysis Method	Seal Analytical AQ2 Discrete Autoanalyzer using AQ2 method EPA-114-A Rev. 11, a cadmium reduction method with a range of 0.25-15 mg N L^{-1}, detection limit of 0.03 mg N L^{-1}.	Seal Analytical AQ2 Discrete Autoanalyzer using AQ400 method EPA-165-A Rev 0, a turbidimetric method with turbidity detection within a range of 5 – 40 mg SO_4 L^{-1}, detection limit of 0.09 mg SO_4 L^{-1}.	Phoenix Doorman 8000 in 2019 (detection limit of 0.1 ppm C; 0-20 ppm standard range) at the USDA National Lab for Agriculture and The Environment and using a Shimadzu TOC-L combustion analyzer (1-50 ppm C) at the McDaniel Lab at ISU for the 2020 and 2021 samples	Shimadzu GC-2014 gas chromatograph using a flame ionization detector for CH_4 and an electron capture detector for N_2O with concentrations calculated using linear regression (CH_4) and quadratic regression (N_2O) of standard concentrations. Calculation of dissolved concentrations following Cawley (2017). Detection limits of 0.09 µL/L (standard range of 0.2-100 µL/L) and 0.11 µL/L (standard range of 0.5-100 µL/L) for N_2O and CH_4, respectively.	
Preservation Method	Concentrated sulfuric acid (1 µL per 1 mL sample), stored at 4°C	Stored at 4°C, analyzed promptly	Concentrated phosphoric acid (1 µL per 1 mL sample), stored at 4°C	If transferred to evacuated vials within 24 h, 0.3 mL of 80% zinc chloride added to the 20 mL glass vial. Else, add 2 mL of 80% zinc chloride to glass BOD bottle.	

2.3 Flow Monitoring

In 2019, inconsistencies with the initial flow monitoring equipment were observed, and the flow was monitored manually using a bucket and stopwatch. At the start of 2020 flow was monitored using vented pressure transducers (Solinst Model 3250 LevelVent; Solinst, Ontario, Canada) installed at the main inlet, outlet A, and outlet B with V-notch. All vented pressure transducers recorded water depth every 15 minutes. The depth of water flowing over the V-notch weir was then converted into a flowrate. Vented pressure transducers at the two chamber outlets were mounted on the V-notch weirs and calibrated at ISU's Agricultural and Biosystems Engineering (ABE) Buss Hydrology Lab to produce a unique equation to convert the depth of water to a flowrate for outlet A and B (Equations 1 and 2), respectively. The V-notch weir in the main inlet was too large to calibrate in ISU's ABE Buss Hydrology Lab; therefore, the flow by-passing in the main inlet was calculated following Dodge et al. (2001). In the main inlet, outlet A, and outlet B, flowrates were calculated every 15 minutes and converted into daily average flowrates. It was assumed that the flow coming into the bioreactor chambers was the same as the flow leaving the bioreactor chambers, which is typical of flow monitoring in these systems (Christianson et al., 2021).

$$Eq.(1): Q(cfs) = 0.2409 * [Pressure\ Transducer\ Reading\ (m)]^{5.8251}$$
$$Eq.(2): Q(cfs) = 0.2745 * [Pressure\ Transducer\ Reading\ (m)]^{5.6109}$$

2.4 Sample Analysis

Methods of analysis for water quality parameters (NO_3-N, TOC, SO_4, dissolved CH_4, and dissolved N_2O) are summarized in Table 1.

2.5 Data Analysis

The HRT of the two chambers was computed by dividing the saturated bioreactor volume (length × width × saturated depth × assumed 70% porosity) by the flow rate. Concentration-

based and flow-weighted percent removal (%) as well as the average mass removal rates of NO_3-N (g NO_3-N m^{-3} d^{-1}) were calculated for each bioreactor chamber and year and for SO_4 (g SO_4 m^{-3} d^{-1}) in 2021. To compute the removals, the concentrations were linearly interpolated between sample collection dates. Concentration-based percent removals were then computed, comparing the main inlet concentration to the two bioreactor chamber's outlet concentrations. Daily average flowrate was used to compute the flow-weighted percent removal and mass removal rate. Flow-weighted percent removal was calculated by multiplying the concentration at the main inlet and outlets by the flowrate leaving the two bioreactor chambers, assuming the flow into the bioreactor is equal to the flow leaving the bioreactor. The entire volume of the bioreactor is used to determine the mass removal rate, by comparing the removal from the main inlet to the two outlets. Lastly, the average and median concentration reduction was computed by comparing the average and median concentrations at the main inlet to the chamber outlets.

Average volume-based production rates of CH_4-C (g CH_4-C m^{-3} d^{-1}) and N_2O-N (mg N_2O-N m^{-3} d^{-1}) were computed in a similar manner, by comparing the rates of production from the main inlet to the two outlets instead of removal. Production rates were converted to an area-based production rate by multiplying the volume-based rates by the bioreactor woodchip depth. Fractional N_2O-N yield of denitrification was computed by dividing the N_2O-N volume-based production rates by the NO_3-N reduction rates for each chamber. Lastly, production rates of CH_4-C and N_2O-N were converted to carbon dioxide equivalents (CO_2e) to allow for investigation of the climate change impact from the bioreactor chambers using 100-y global warming potentials of 28 and 265, respectively (Myhre et al., 2014). The CO_2e load assumes that these gases will be completely emitted from downstream waters to the atmosphere, as suggested by prior studies of drainage water where N_2O was degassed within meters of tile drain outfalls (Reay et al., 2003).

2.6 Statistical Analysis

Variability in the median concentrations of NO_3-N, TOC, SO_4, dissolved CH_4-C, and dissolved N_2O-N by location across the bioreactor chamber's length and width were explored using an inverse distance weighting method in RStudio software package with R version 4.1.0 (R Core Team, 2019). This method was used to interpolate the concentrations throughout the bioreactor using the observed concentrations at the sampling locations and a weighting factor of 2.5; inverse distance weighting has previously been used in wetland and surface water studies (e.g., Jia & Yan, 2018; Khouni et al., 2021). This analysis was completed with the gstat (Pebesma et al., 2015) and stars (Pebesma et al., 2020) packages in RStudio while the data visualizations from the inverse distance weighting interpolation were generated in RStudio using the Tidyverse (Wickham & Wickham, 2019) and patchwork (Pedersen, 2020) packages. The main inlet and outlet NO_3-N, SO_4, CH_4-C, and N_2O-N concentrations and the flow-weighted concentrations for each chamber were compared using a Wilcoxon signed-rank test ($p < 0.05$) using RStudio. Similarly, the outlet concentrations of NO_3-N, SO_4, CH_4-C, and N_2O-N were compared using a Wilcoxon signed-rank test ($p < 0.05$) using RStudio.

3. Results and Discussion

3.1 Overall Bioreactor Performance

3.1.1 Flow Conditions

Flow conditions are summarized for the monitoring periods in 2020 and 2021 in Fig. 2. The first year of monitoring, 2019, was excluded from this analysis due to differences in flow monitoring equipment and techniques. During the two years of flow monitoring, the flowrate never reached the designed flowrate and consistently low flowrates were observed in both bioreactor chambers. In chamber A, the median flow from 2020 and 2021 was observed to be 0.236 L s^{-1} (mean of 0.433 L s^{-1}) or 4.50% of the designed capacity while in chamber B, the

median flow was observed as 0.379 L s^{-1} (mean of 0.578 L s^{-1}) or 7.22% of the designed capacity. Low flows observed in 2021 were exacerbated by drought conditions, with an annual precipitation of 717 mm compared to the 30-y average (1981-2010) of 935 mm in Ames, Iowa (Daigh et al., 2015). In Chamber A, these flow rates corresponded to HRTs ranging from 16.9–121 h in 2020 (median of 49.6 h) and 31.6–90.4 h in 2021 (median of 64.3 h). In Chamber B, the HRTs ranged from 19.0–135 h in 2020 (median of 46.0 h) and 19.2–72.5 h in 2021 (median of 38.3 h). In 2020, the stoplogs were adjusted in the chamber inlets to try to maintain equal flow between the two chambers. It became apparent that consistently equal flow was not possible between the two chambers regardless of stoplog configuration, due to varying inlet elevations. As a result, the chamber inlets and outlets were configured the same for the 2021 season. Chamber B tended to have higher flow rates than chamber A (Figure 2), especially in 2021, due to inlet B being located at a slightly lower elevation than inlet A. This trend was more pronounced in 2021 due to the ongoing drought conditions, stoplog configuration, and generally lower flowrates to the system that year. As a system in the natural environment, large fluctuations in flow from year to year can occur.

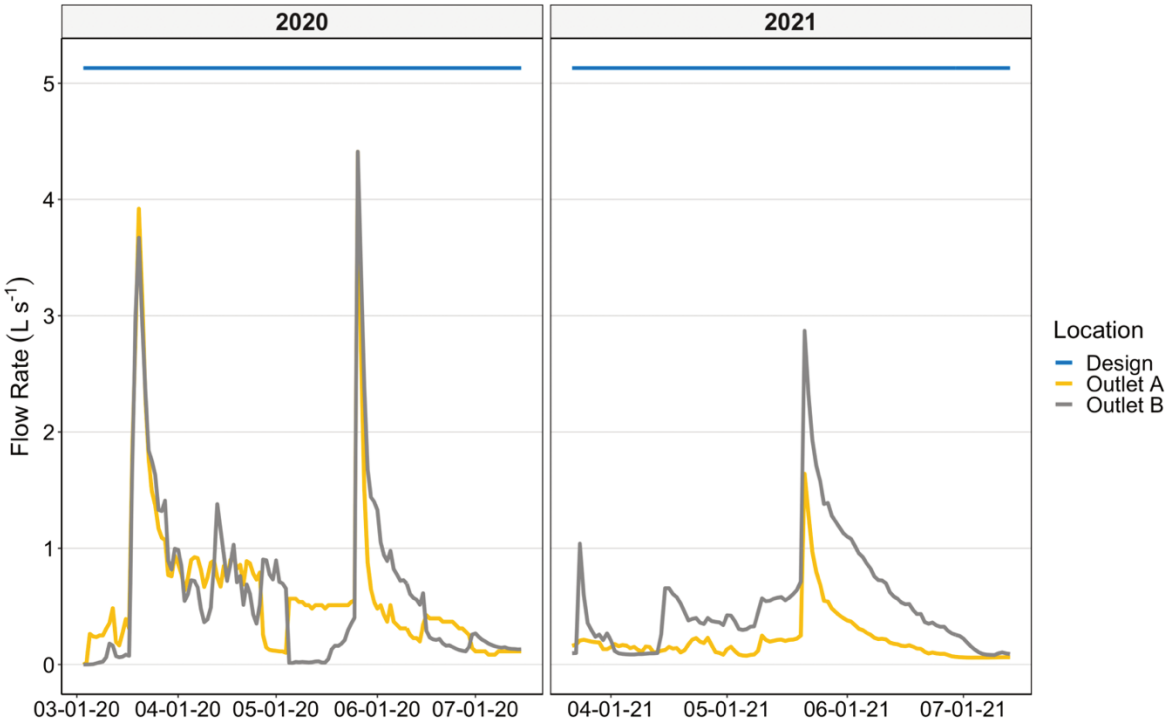

Figure 2. Low flow conditions were consistently observed in both bioreactor chambers. Chamber A (yellow) typically experienced lower flowrates than chamber B (gray), both of which experienced lower flowrates than designed (blue). Note that a period of no flow occurred between summer 2020 and spring 2021. Another period of no flow occurred mid-summer 2021 through the spring 2022 (which was outside this study's monitoring period).

3.1.2 Mass Removal and Production

In 2020, the bioreactor system received 203 kg NO_3-N, with 37 kg NO_3-N by-passing the bioreactor untreated. Chamber A and chamber B received 90 kg NO_3-N and 76 kg NO_3-N, respectively. Over 80% of the flow to the bioreactor was treated (less than 20% by-passed). Within chamber A and chamber B, 72 kg NO_3-N and 61 kg NO_3-N were removed in 2020, respectively (17 kg NO_3-N and 15 kg NO_3-N left chamber A and chamber B, respectively). In 2021, the bioreactor system received 76 kg NO_3-N, with none of the NO_3-N by-passing. Chamber A and chamber B received approximately 20 kg N and 56 kg N, respectively. All of the flow to the bioreactor was treated by the bioreactor system in 2021 (0% of the flow was by-passed). Within chamber A and chamber B, 17 kg NO_3-N and 33 NO_3-N were removed, respectively (3 kg NO_3-N and 23 kg NO_3-N left chamber A and chamber B, respectively).

Flowrate is directly correlated with the HRT in these systems (Tchobanoglous et al., 2003). The longer the residence time, the greater the percent removal of NO_3 that can be expected, as this provides additional time for denitrifying bacteria to convert NO_3-N to N_2 gas (Christianson et al., 2012). Consistently low flowrates observed often resulted in long HRTs, high percent removals of NO_3-N, and low mass removal rates of NO_3-N (Table 2). The mass removal rates of NO_3-N (ranging from 0.73 to 1.33 g NO_3-N removed m^{-3} d^{-1}) are lower than several other bioreactor studies; two reviews of bioreactor performance have reported mean NO_3-N mass removal rates of 4.7 g NO_3-N m^{-3} d^{-1} (Addy et al., 2016) and 7.2 g NO_3-N m^{-3} d^{-1} (median of 5.1 g NO_3-N m^{-3} d^{-1}) (Christianson et al., 2021). However, the lower mass removal rates were anticipated due to the bioreactor size, with a large volume of unused woodchips in each chamber, and due to the system often being N limited. Significant reduction ($p < 0.01$) of NO_3-N was observed in each chamber every year with an average magnitude of reduction of 8.6-11.1 mg NO_3-N L^{-1} (Table 2). In 2021, the lower flowrates and higher HRTs in Chamber A allowed for more NO_3-N removal and higher percent removal of NO_3-N (Table 2); for these reasons, chamber B tended to have greater NO_3-N concentrations leaving the bioreactor (with lower percent removal of NO_3-N, Table 2).

Table 2. Summary of the average percent and mass removal rate of nitrate-N (NO_3-N) in chambers A and B in 2019, 2020, and 2021 and the magnitude of the average and median concentration reductions observed.

NO_3-N	**Chamber A**			**Chamber B**		
	2019	**2020**	**2021**	**2019**	**2020**	**2021**
Average Concentration-based Percent Removal (%)	98.9%*	90.0%*	94.2%*	94.5%*	85.6%*	72.0%*
Flow-weighted Percent Removal (%)	---	80.8%*	85.0%*	---	80.7%*	59.7%*
Average (Median) Magnitude of Concentration Reduction (mg L^{-1})	11.1 (11.8)	11.4 (11.6)	11.1 (12.5)	10.6 (11.8)	10.8 (11.4)	8.6 (10.6)
Mass Removal Rate (g NO_3-N m^{-3} d^{-1})	---	1.33	0.73	---	1.33	1.07

*Denotes significant reduction of NO_3-N with $p < 0.01$ using Wilcoxon-signed rank tests.

Removal of SO_4 was also observed, primarily in chamber A (Table 3). The removal of SO_4 observed in chamber A is similar to other bioreactor studies experiencing SO_4-reducing conditions where SO_4 removal has ranged from 25% to 56% while the NO_3-N removal has ranged from 81% to 96% (David et al., 2016; Shih et al., 2011). Chamber A's SO_4 loss was significant ($p < 0.01$) with an average of 5.18 mg SO_4 L^{-1} removed (median of 4.98 mg SO_4 L^{-1} removed). Average incoming SO_4 concentrations were 12.3 mg SO_4 L^{-1} and 11.9 mg SO_4 L^{-1} for chambers A and B, respectively. In contrast to chamber A, there was no evidence of significant SO_4 removal in chamber B ($p = 0.40$) (Table 3), likely due to higher NO_3-N concentrations within that chamber limiting the SO_4 removal, as that process is further down the redox potential ladder (Chapin et al., 2011; Voroney & Heck, 2015). A similar pattern was observed in another bioreactor study, with temporal differences in sulfate removal patterns being attributed to the varying nitrate concentrations leaving the bioreactor which were dominated by the HRTs experienced in that study (Rivas et al., 2020). Mass removal rates of SO_4 from bioreactors have not been previously reported to the best of our knowledge, and in our study, they ranged from 0.02 g SO_4 m^{-3} d^{-1} in chamber B to 0.23 g SO_4 m^{-3} d^{-1} in chamber A (Table 3). The rates of sulfate removal observed in these chambers were similar in magnitude to observations from stream sediments and other freshwater systems (e.g., Marvin-DiPasquale et al., 2009; Pester et al., 2012).

Table 3. Summary of sulfate (SO_4) removal metrics and dissolved nitrous oxide (N_2O) and methane (CH_4) production metrics.

Parameter		2021	
		Chamber A	**Chamber B**
SO_4^{2-}	Concentration-based Percent Removal (%)	40.8%*	4.56%
	Flow-weighted Percent Removal (%)	25.5%*	0.87%
	Mass Removal Rate (g SO_4 m^{-3} d^{-1})	0.23	0.02
N_2O-N	Fractional N_2O-N Yield of Denitrification	-0.03%	0.03%
	Flow-weighted Concentration Entering Chamber (μg N_2O-N L^{-1})	8.99	8.10
	Flow-weighted Concentration Leaving Chamber (μg N_2O-N L^{-1})	5.98	10.5

	Volume-based Production Rate (mg N_2O-N m^{-3} d^{-1})	-0.20	0.34
	Area-based Production Rate (mg N_2O-N m^{-2} d^{-1})	-0.21	0.36
CH_4-C	Flow-weighted Concentration Entering Chamber (μg CH_4-C L^{-1})	13.2	9.95
	Flow-weighted Concentration Leaving Chamber (μg CH_4-C L^{-1})	7,978	506
	Volume-based Production Rate (g CH_4-C m^{-3} d^{-1})	0.54	0.07
	Area-based Production Rate (g CH_4-C m^{-2} d^{-1})	0.58	0.07

*Denotes significant reduction of SO_4 with $p < 0.01$ using Wilcoxon-signed rank tests.

In a similar manner, production rates of N_2O-N and CH_4-C were calculated (Table 3). In chamber A, removal of N_2O-N was documented, while in chamber B, production of N_2O-N was observed, both of which were significant ($p < 0.01$). In the microbial denitrification process (conversion of NO_3 to N_2 gas), N_2O is an intermediate step, which is why increased levels of N_2O can be observed leaving a bioreactor. Under complete denitrification, N_2O would be further reduced to N_2 gas by the denitrifying bacteria (Knowles, 1982), which is why we can see lower N_2O concentrations leaving bioreactors. Removal of dissolved N_2O-N has been observed previously (Audet et al., 2021; Fenton et al., 2016; Manca et al., 2020; Rivas et al., 2020) and has been attributed to NO_3 limiting conditions (Manca et al., 2020). The production observed in chamber B (0.34 mg N_2O-N m^{-3} d^{-1}) is within the range recently observed (0.01–15.25 mg N_2O-N m^{-3} d^{-1}) in another bioreactor study (Audet et al., 2021). Average N_2O-N concentrations leaving chambers A and B were 5.98 μg N_2O-N $L^{-1}$and 10.5 μg N_2O-N L^{-1}, respectively (Table 3), falling within the range of several other bioreactor studies (Audet et al., 2021; Manca et al., 2020; Manca et al., 2021; Moorman et al., 2010; White et al., 2022). In chamber B, where N_2O-N increased from the inlet to the outlet of the bioreactor, the N_2O-N accounted for less than 0.1% of the NO_3-N removed. This N_2O production is very small, especially in comparison to the Intergovernmental Panel on Climate Change default emission factor for N_2O production from groundwater (EF5g), which estimates that 0.60% of N leached from agricultural soil will be emitted as N_2O-N from degassing of groundwater (Hergoualc'h et al., 2019). Comparing the total incoming NO_3-N and dissolved N_2O-N (estimated total leached N) to the dissolved N_2O-N

leaving the bioreactor, 0.07% of the leached N was emitted as N_2O-N. A recent bioreactor study similarly observed an average of 0.23% of NO_3 removed as N_2O, again lower than the default emission factor for N_2O production from groundwater (White et al., 2022). Previous studies demonstrated the majority of N_2O emissions from bioreactors (76% – 99.9%) are released in drainage water rather than through the bioreactor surface (Davis et al., 2019; Manca et al., 2021; Warneke et al., 2011) and therefore dissolved N_2O was the only flux monitored in this study. Due to the low fraction of dissolved N_2O-N leaving the bioreactor relative to the incoming NO_3-N and N_2O-N and the EF5g default emission factor, bioreactors could be considered for inclusion as a climate smart agriculture practice. These climate smart practices are described as reducing GHG emissions while also maintaining or improving yields (FAO, 2022).

When considering the CH_4-C production, both chambers acted as a significant ($p < 0.01$) source of dissolved CH_4-C (Table 2). In chamber B, a low production rate was observed (0.07 g CH_4-C m^{-3} d^{-1}), which was below the range of production rates previously observed in another study (0.51–1.69 g CH_4-C m^{-3} d^{-1}) (Davis et al., 2019). The production rate in chamber A (0.54 g CH_4-C m^{-3} d^{-1}) was within the range observed in that previous study. Average concentrations leaving the two bioreactor chambers were 7,978 μg CH_4-C L^{-1} and 506 μg CH_4-C L^{-1} for chamber A and B, respectively, which fall within the range of previous studies (5.28–18,000 μg CH_4-C L^{-1}) (Davis et al., 2019; Fenton et al., 2016; Warneke et al., 2011).

Mass removal and production rates are common metrics to assess bioreactor performance (Christianson et al., 2021; Christianson & Schipper, 2016) by providing an overall idea of the rate at which pollutants are either removed or produced. This is an important measure in identifying the impact the bioreactor can have on meeting nutrient reduction goals and allowing for comparison across bioreactor studies where variable performance can be seen due to

variations in temperature, incoming NO_3-N concentrations, HRTs, carbon availability, etc. (Addy et al., 2016; Christianson et al., 2012). However, this method of analysis does not allow for thorough investigation into the bioreactor design, including spatial pollutant removal or production, and temporal performance including the performance relative to HRTs, which are important factors needed to improve bioreactor design.

3.2 Spatial Nitrate Concentrations Over Time

Results were evaluated to assess the spatiotemporal bioreactor performance to identify both the regions of the bioreactors where NO_3-N was being removed and how this varied over time. Median NO_3-N concentrations observed in each bioreactor chamber over time are represented in Figure 3 using an inverse distance weighting interpolation method. In 2019, chamber A and chamber B both had high NO_3-N removal with near complete NO_3-N removal at approximately 10 m (or 27%) into the chamber's length (Fig. 3). In 2020, while the NO_3-N concentration observed was typically higher throughout the bioreactor chamber, likely due to the greater flow conditions (Fig. 2), near complete NO_3 removal was still observed by 30 m (or 82%) into the chamber's length for both chamber A and chamber B (Fig. 3). In contrast, the median NO_3-N concentration in chamber A and chamber B were more variable in 2021 (Fig. 3). The higher NO_3-N concentrations in chamber B in 2021 compared to chamber A are likely due to the higher flow conditions observed in chamber B (mean flow 2.45 times greater in chamber B than chamber A; median flow 2.38 times greater in chamber B than chamber A in 2021) (Fig. 2). The drought conditions in 2021 contributed to the pronounced differences in chambers A and B as the chamber B inlet was unintentionally installed at a slightly lower elevation than the chamber A inlet; therefore, more flow went to chamber B under the low flow conditions experienced.

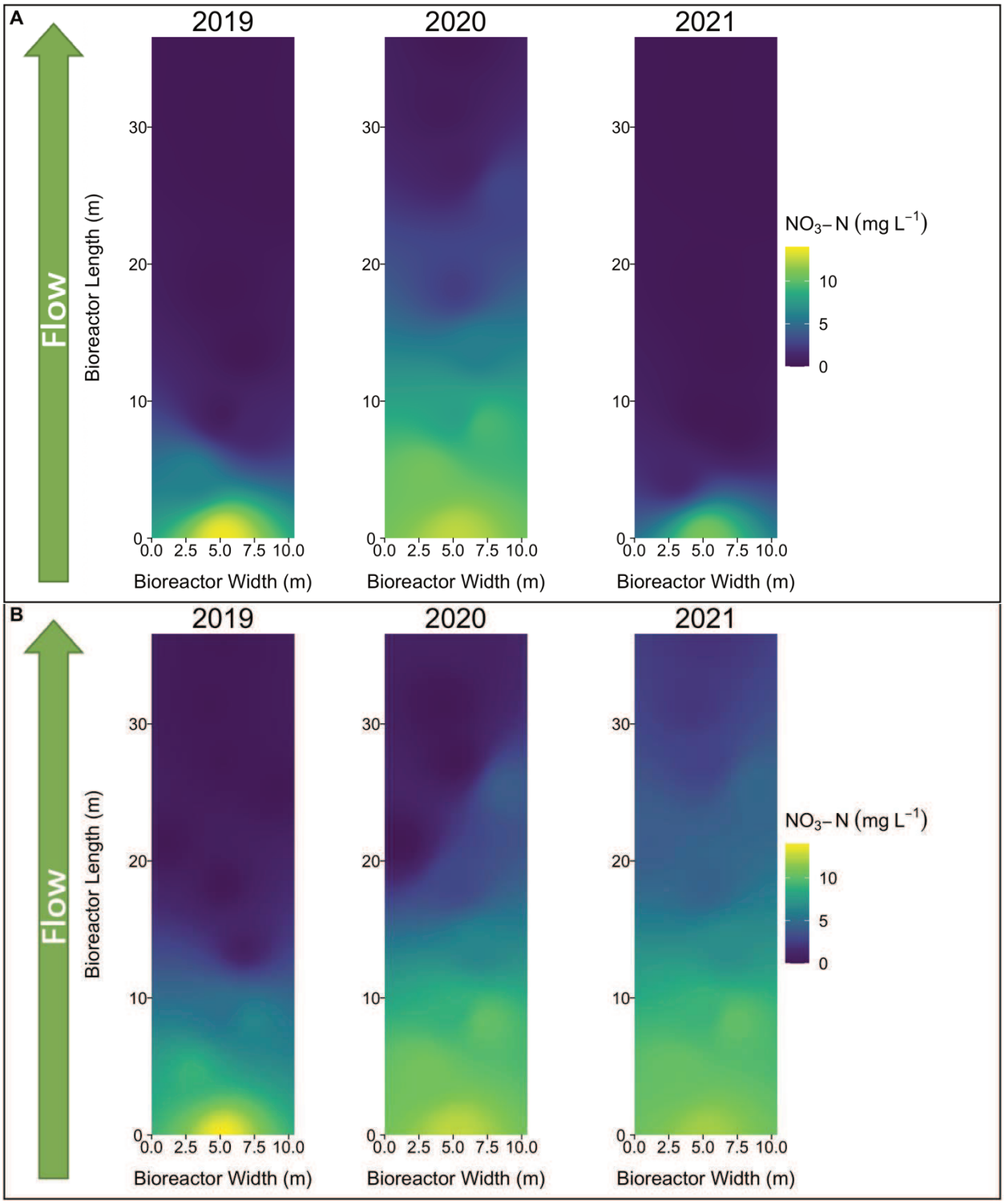

420 Figure 3. Median spatial nitrate-N (NO_3-N) concentrations in (A) chamber A and (B) chamber B
421 over time. The direction of the flow is indicated, and the bioreactor dimensions are displayed in
422 units of m across the bioreactor length and width.

Assessment of the spatiotemporal dynamics of NO_3-N removal in the dual chamber bioreactor allow for a deeper understanding of the bioreactor performance by documenting at what point in the system the NO_3-N has reached essentially complete removal. Further, previous bioreactor studies have documented that bioreactor performance is greater (higher removal rate of NO_3-N) in the first two years of operation (Addy et al., 2016). This study observed a similar trend in chamber B over time, with the highest NO_3-N removal in the first year of operation (2019), with lower percent NO_3-N removal in each of the following years (average concentration reductions of 94.5% in the first year to 72.0% in the third year of operation; Table 2). Most bioreactor studies have evaluated the performance of relatively new bioreactors. Spatiotemporal dynamics observed, especially in chamber B, demonstrate a need for long-term performance studies and consideration of bioreactor design in terms of long-term NO_3-N removal. Future work of spatiotemporal NO_3-N dynamics could be used to quantify how the bioreactor performs under a variety of conditions (e.g., in normal, wet, and drought years) and time periods which could further future recommendations for the bioreactor design standard.

3.3 Spatial TOC Concentrations over Time

An initial flush of excess C leaving bioreactors is often observed upon system startup, after which, C leaving the system often rapidly declines (Greenan et al., 2009; Hoover et al., 2016). In 2019, TOC concentrations generally increased from the bioreactor inlet to the outlet (Fig. S1). In both chambers, it was observed that the TOC concentration decreased rapidly following 2019, with much lower concentrations observed in both 2020 and 2021 (Fig. S1). This observation of lower TOC concentrations over time is consistent with other bioreactor studies (David et al., 2016; Hoover et al., 2016).

Future work could evaluate the C/N ratios of the woodchips spatially within the bioreactor. Significantly higher C/N ratios of woodchips near the outlet when compared to near the inlet have been observed in bioreactor studies, indicating that as the bioreactor ages, the regions near the inlet of the bioreactor may become depleted of C or enriched in N, requiring recharge (replacement of the woodchips) sooner than the rest of the bioreactor (Ghane et al., 2018; Schaefer et al., 2021). Woodchip C/N ratios have been used as an explanatory variable of the woodchip degradation and quality with lower C/N ratios observed in aged woodchips resulting from decreased C content and increased N (Ghane et al., 2018; Moorman et al., 2010). The remaining C has also been observed to be more recalcitrant, with lower quality C remaining (Ghane et al., 2018). Recently, partial bioreactor recharge near the inlet of the bioreactor has been proposed (Schaefer et al., 2021). However, long-term monitoring of partial bioreactor recharges would be needed to understand the lifespan of the rest of the bioreactor. The inlet region of the bioreactor can be subjected to large fluctuations in the saturation level which can result in periods of drying and rewetting of the woodchips. This has been hypothesized to enhance the breakdown of the woodchips and shorten the bioreactor life (Ghane et al., 2018; Maxwell et al., 2019). Minimizing these conditions could improve bioreactor lifespan. Combined with spatiotemporal dynamics of NO_3-N, the design of these systems could potentially be optimized to provide a better longevity and NO_3-N removal.

3.4 Biogeochemical Processes and Dynamics within the Bioreactor

Nitrate removal within bioreactors may result in higher rates of biogeochemical processes occurring at lower redox states. Limiting SO_4 reduction in bioreactors may be important in the design and management of these systems due to its link to methylmercury production (Gilmour et al., 1992; Gilmour et al., 2013). However, due to the similarity in sulfate reduction rates to other freshwater systems (Marvin-DiPasquale et al., 2009; Pester et al., 2012) and the small

relative footprint of bioreactors, it is unknown if bioreactors would have a measurable impact on methylmercury levels at the catchment scale. Other constituents monitored in this study were dissolved CH_4 and N_2O, which are both of concern as these are known contributors to global warming with a global warming potential 28 and 265 times greater than carbon dioxide, respectively (Myhre et al., 2014).

3.4.1 Spatial Biogeochemical Processes and Dynamics

The median concentrations of NO_3-N, SO_4, dissolved CH_4-C, and dissolved N_2O-N were investigated to evaluate the spatial pollutant dynamics within the two bioreactor chambers (Fig. 4). Long HRTs due to the lower flow conditions in chamber A allowed for removal of N_2O-N from the inlet to the outlet of the bioreactor as well as near complete NO_3-N removal at approximately 10 m (or 27%) into Chamber A (Fig. 4A). This essentially complete NO_3-N removal potentially allowed for conditions under which additional biogeochemical reactions could occur. Near the region where NO_3-N was nearly removed, SO_4 was also removed (approximately at 10 m or 27% into the bioreactor length). Similarly, as SO_4 removal began to occur, CH_4-C was also produced. In chamber B, the higher flow conditions (Fig. 2) and NO_3-N concentrations have greatly inhibited SO_4 removal and CH_4 production but allowed for a slight increase in the outlet dissolved N_2O-N concentrations compared to the inlet (Fig. 4B). As a result of the higher NO_3-N concentrations from greater flow rates in chamber B (median outlet concentration of 1.97 mg NO_3-N L^{-1}) compared to chamber A (median outlet concentration of

0.125 mg NO_3-N L^{-1}), both the removal of SO_4 and the production of CH_4-C were greatly limited.

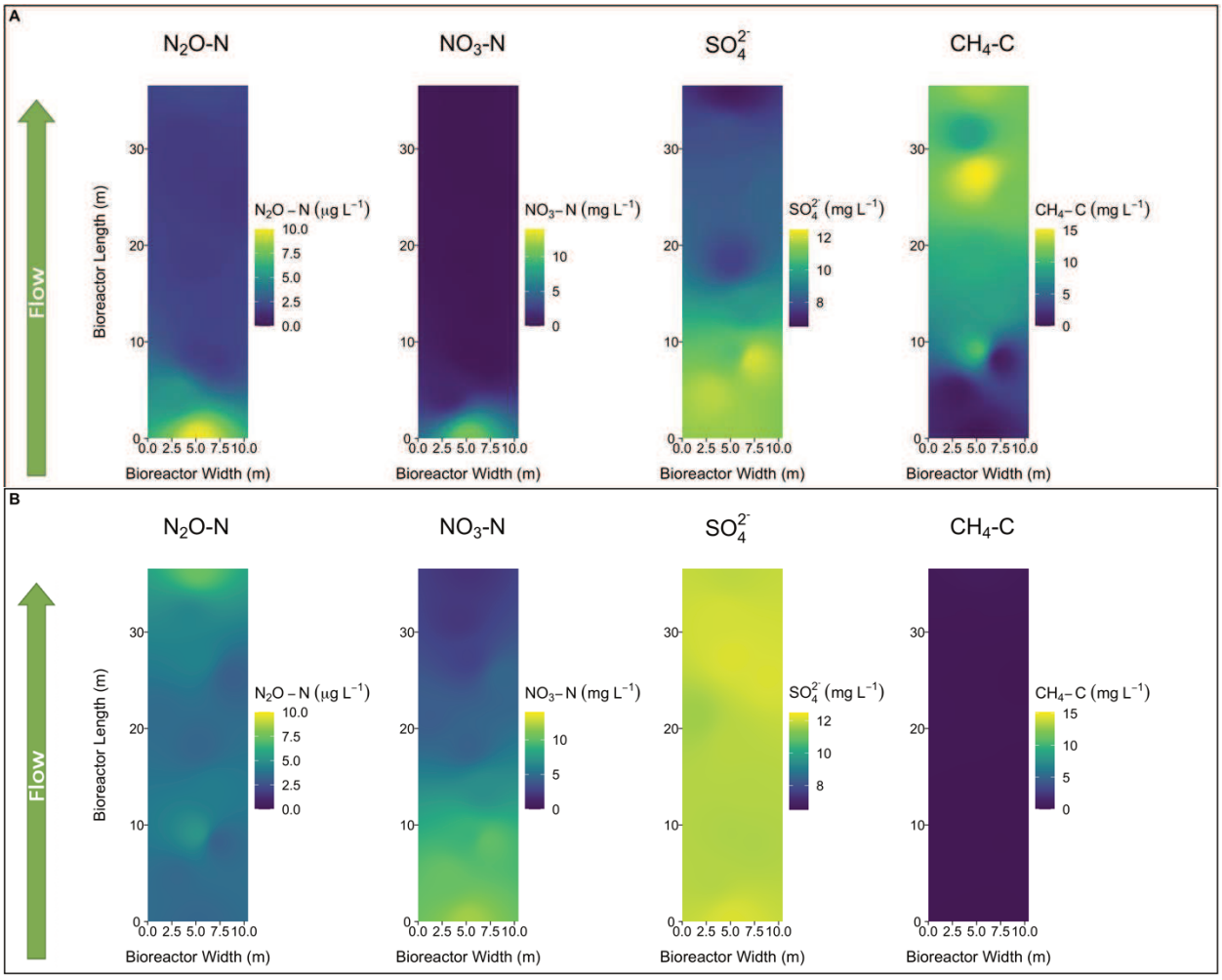

Figure 4. Spatial multi-pollutant dynamics within (A) chamber A and (B) chamber B. The median concentrations of N_2O-N, NO_3-N, SO_4, and CH_4-C are represented. The direction of the flow is indicated, and the bioreactor dimensions are displayed in units of m across the bioreactor length and width. Note that the SO_4 scale does not go to zero to allow for the gradient in concentrations to be better observed.

Investigating the spatial distributions of chemical species within bioreactors allows for a greater understanding of the relationship among different pollutants, such as when and where they are removed or produced in the system. From the results in Chamber B, maintaining a NO_3-N concentration at or above ~2 mg NO_3-N L^{-1} minimizes the removal of SO_4 and production of

500 CH_4 and could be used as management strategy to reduce the risks of these processes from
501 occurring. By maintaining these NO_3-N concentrations, the redox potential can be kept at a level
502 where the energy return for CH_4 production or SO_4 removal are unfavorable for the microbes in
503 the bioreactor, limiting any changes in the concentrations of CH_4 or SO_4 (Chapin et al., 2011;
504 Voroney & Heck, 2015).

505 **3.4.2 Biogeochemical Processes by HRT**

506 Improving the design of bioreactor systems to limit the risk of undesired biogeochemical
507 reactions is critical to ensuring the long-term sustainability and adoption of bioreactors. One
508 design criterion that has previously been recommended as a control for N_2O-N and CH_4-C
509 production is the HRT, with a previous study recommending an HRT in the range of 6-8 h to
510 limit the global warming contributions from both N_2O and CH_4 (Davis et al., 2019). Other
511 bioreactor studies have also observed a relationship between HRT and other biogeochemical
512 processes with short HRTs increasing the risk of N_2O production and long HRTs increasing the
513 risk of CH_4 production or SO_4 removal (Jéglot et al., 2022; Rivas et al., 2020). Here, we
514 investigate the dynamics of multiple pollutants by several ranges of observed HRTs in the dual-
515 chamber bioreactor, combining the data from both chamber A and chamber B. The observed
516 outlet concentrations for NO_3-N, SO_4, CH_4-C, and N_2O-N by HRT are summarized (Fig. 5).

517 When considering trends in dissolved N_2O-N concentrations, HRTs of <50 h resulted in
518 significantly ($p < 0.01$) higher outlet concentrations of N_2O-N (median of 8.86 μg N L^{-1}; mean of
519 10.74 μg N L^{-1}) while HRTs above 50 h decreased N_2O-N outlet concentrations to approximately
520 2 μg N_2O-N L^{-1} (median of 1.87 μg N L^{-1}; mean of 2.13 μg N L^{-1}). In terms of NO_3-N,
521 significantly higher outlet concentrations ($p < 0.01$) were observed at HRTs of <50 h (median of
522 2.39 mg NO_3-N L^{-1}; mean of 3.66 mg NO_3-N L^{-1}) than at HRTs >50 h (Fig. 5). At HRTs above

523 50 h, near-complete removal of NO_3-N was observed (median outlet concentration of 0.13 mg
524 NO_3-N L^{-1}; mean of 0.19 mg NO_3-N L^{-1}). SO_4 removal was limited to HRTs above 60 h, where
525 complete removal of NO_3-N was observed; however, significant differences in outlet SO_4
526 concentrations were again observed above and below an HRT of 50 h. At HRTs <50 h, the
527 median outlet SO_4 concentration was 11.9 mg L^{-1} (mean of 12.2 mg L^{-1}), while at HRTs >50h,
528 the median outlet concentration was 5.61 mg L^{-1} (mean of 6.8 mg L^{-1}). Lastly, when considering
529 the production of CH_4-C, a significant increase ($p < 0.01$) in the outlet concentration was
530 observed at HRTs >50 h (median of 9.61 mg L^{-1}; mean of 10.6 mg L^{-1}) compared to at HRTs
531 <50 h (median of 0.34 mg L^{-1}; mean of 0.57 mg L^{-1}).

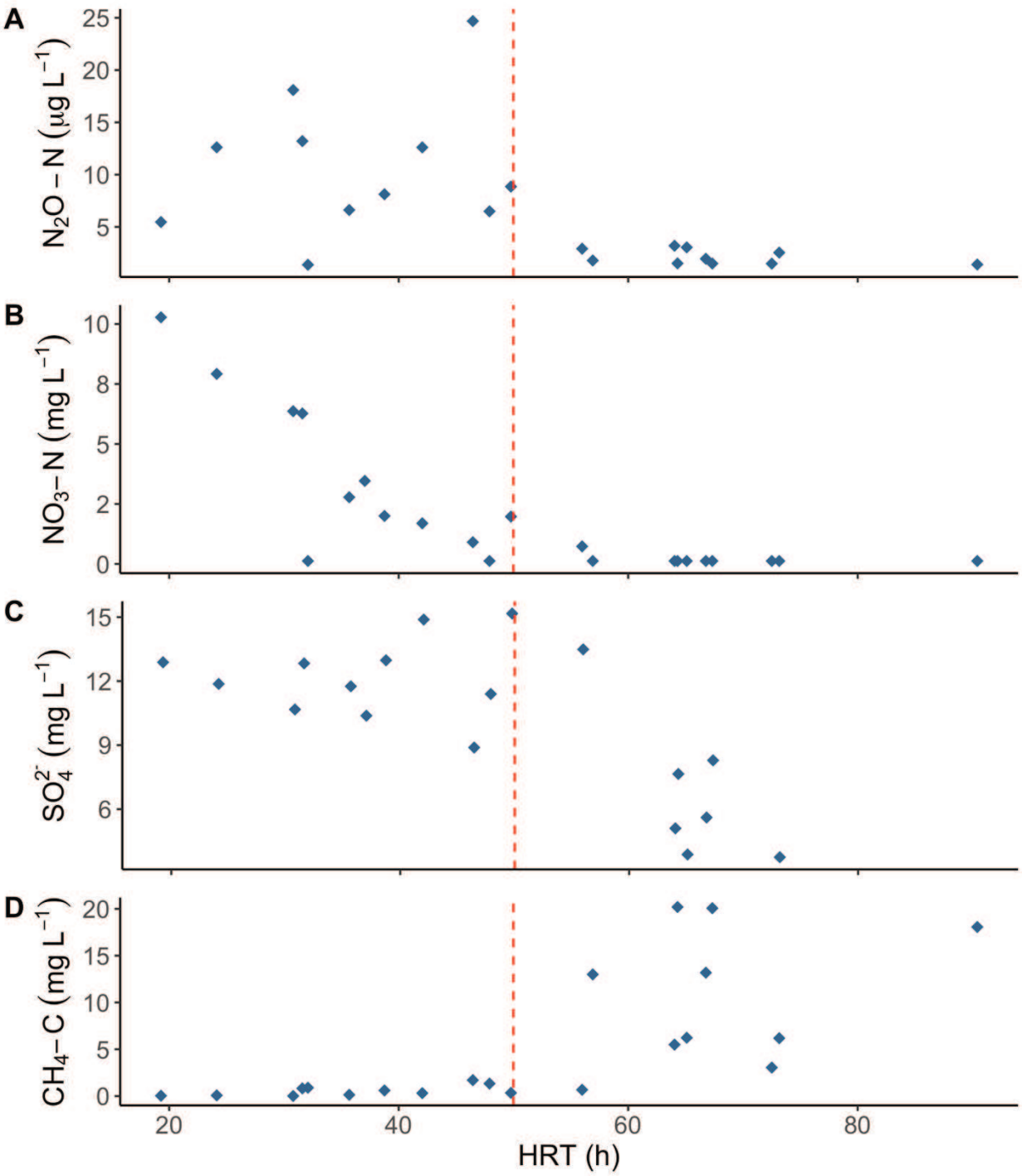

Figure 5. Multi-pollutant dynamics by HRT. Outlet concentrations of N_2O-N, NO_3-N, SO_4, and CH_4-C are represented here. The red-dashed line represents an HRT of 50 h. Significant differences above and below an HRT of 50 h were observed ($p < 0.01$) for all pollutants. Note, there were four missing samples for SO_4^{2-} (two per chamber) that could not be analyzed within the method holding period.

3.4.3 Implications of Bioreactor Biogeochemical Reactions

To understand the overall global warming contributions from the bioreactor system, the production rates of N_2O-N and CH_4-C were converted to CO_2e. The volume-based production rates in chambers A and B were 20.1 g CO_2e m^{-3} d^{-1} and 2.75 g CO_2e m^{-3} d^{-1}, respectively, and were largely dominated by CH_4-C emissions. A previous study observed a range of CO_2e loads in bioreactors operated at HRTs of 2, 8, and 16 h of 63.56 – 241.06 g CO_2e m^{-3} d^{-1}, which are greater than the loads observed in either chamber A or B (Davis et al. 2019). On an area-basis, the CO_2e loads were 21.4 g CO_2e m^{-2} d^{-1} and 2.94 g CO_2e m^{-2} d^{-1} from chambers A and B, respectively. These daily areal production rates were converted to annual production rates by multiplying the daily rates by the days of flow in 2021. On an annual basis, the production rates were 11,984 kg CO_2e ha^{-1} y^{-1} and 2,264 kg CO_2e ha^{-1} y^{-1} for chambers A and B, respectively. For comparison, a typical agricultural field under corn/soybean rotation located several km from the bioreactors emitted ~3,700 kg CO_2e ha^{-1} y^{-1} as N_2O (Lawrence et al., 2021). Chamber A was observed to have prolonged HRTs (median of 64 h in 2021) and CO_2e loads of ecological significance (11,984 kg CO_2e ha^{-1} y^{-1}), being greater than what is observed in poorly drained row crop agriculture fields. In contrast, Chamber B with lower HRTs (median of 39 h in 2021) and higher outlet NO_3-N concentrations near 2 mg NO_3-N L^{-1} had CO_2e loads lower than the nearby agricultural field (2,264 kg CO_2e ha^{-1} y^{-1}) (Lawrence et al., 2021). Combining this information with the biogeochemical processes by HRT ranges, HRTs above 50 h should be avoided in these bioreactor systems. However, considering the small spatial footprint of the bioreactors (~0.1 ha) relative to the estimated area of drainage water treated (~37 ha), even in the case of the long HRT bioreactor, the increased GHG production is negligible at landscape scale. Nitrate was almost entirely removed from water draining ~37 ha, while total GHG emissions increased by only 1% over these 37 ha.

562 The current design standard for bioreactor systems was modified to require an orifice at
563 the outlet water control structure of the bioreactor to allow for the chamber to drain within 48 h
564 during low or no flow conditions (NRCS, 2020). This study supports that the current design
565 standard method, with an orifice to drain the bioreactor in a 48-h period, reduces the risk of
566 unintended byproducts and pollution swapping from occurring under similar environmental
567 conditions as this study. Global warming contributions from bioreactors at shorter HRTs are
568 often dominated by N_2O-N emissions, which are more potent than CH_4-C. A previous study
569 suggested extending the minimum HRT to 6 h in the bioreactor design standard (Davis et al.,
570 2019); our study supports and builds on this suggestion by also providing a recommendation of
571 the maximum HRT. In the context of dual-chamber bioreactors, the system could also be
572 managed to only use one of the parallel chambers under traditional or low-flow conditions and
573 use the second chamber under higher-flow conditions.

574 **4. Conclusions**

575 Consistent low-flow conditions observed in our dual-chamber bioreactor system resulted
576 in prolonged HRTs, complete NO_3-N removal on numerous occasions, and the potential for SO_4
577 removal and CH_4-C production to occur. Through this study, a target NO_3-N concentration of ~2
578 mg NO_3-N L^{-1} (the median concentration at the outlet of chamber B in 2021) is proposed to
579 prevent SO_4 removal and rapid CH_4-C production from occurring. Additionally, avoiding HRTs
580 above 50 h may reduce the risk of pollution swapping from occurring as well as the global
581 warming potential from these systems. This observation aligns with the current design standard
582 recommendation of designing bioreactors with an orifice to drain the bioreactor within 48 h.
583 However, even under extreme low-flow conditions, the landscape-scale impact of pollution
584 swapping was determined to be small relative to the benefits of NO_3 removal from the
585 bioreactors. Under the worst-case scenario, GHG emissions increased <1% when expressed over

586 the drainage area treated by the bioreactor, but >72% of the NO_3 was removed from the water
587 draining this landscape. Sulfate removal also occurred but was within the range of previous
588 observations from freshwater wetlands and stream sediments, suggesting that the impact of
589 bioreactors on catchment-scale sulfate reduction would likely be small. Future work could
590 evaluate the spatiotemporal NO_3-N removal to quantify how a bioreactor performs under a
591 variety of conditions (e.g., in normal, wet, and drought years) and time periods. This work could
592 be combined with spatiotemporal monitoring of the woodchip C/N ratios to identify strategies to
593 improve the bioreactor design standard or to evaluate the possibility of partial bioreactor
594 recharges. The results of this study could be used globally to guide the management of these
595 systems to prevent pollution swapping, especially for systems treating subsurface drainage.
596 Future work could be conducted to identify similar management recommendations for
597 bioreactors treating alternative nitrate laden water sources.

598 **Acknowledgements**

599 The authors thank Leigh Ann Long for her sample analysis in the Water Quality Research
600 Laboratory, Stephen Potter for his analysis of the TOC samples, Carlos Tenesaca for the
601 dissolved GHG analysis, Ji Yeow Law for his design of the sampling well locations, and Andrew
602 Craig for his assistance with the bioreactor installation and flow monitoring setup. The authors
603 would also like to thank the Iowa State University Research Farm staff for their assistance in
604 managing this site. This material is based upon work supported by the Natural Resources
605 Conservation Service, U.S. Department of Agriculture, under number NR186114XXXXG004.
606 Any opinions, findings, conclusions, or recommendations expressed in this publication are those
607 of the author(s) and do not necessarily reflect the views of the U.S. Department of Agriculture.
608 USDA is an equal opportunity provider and employer. This project was also supported by

609 Agriculture and Food Research Initiative Competitive Grant no. 2018-67016-27578 awarded as a
610 Center of Excellence from the USDA National Institute of Food and Agriculture.

611 **References**

612 Addy, K., Gold, A. J., Christianson, L. E., David, M. B., Schipper, L. A., & Ratigan, N. A.
613 (2016). Denitrifying Bioreactors for Nitrate Removal: A Meta-Analysis. *J Environ Qual*,
614 *45*(3), 873-881. https://doi.org/10.2134/jeq2015.07.0399
615 Audet, J., Jéglot, A., Elsgaard, L., Maagaard, A. L., Sørensen, S. R., Zak, D., & Hoffmann, C. C.
616 (2021). Nitrogen removal and nitrous oxide emissions from woodchip bioreactors
617 treating agricultural drainage waters. *ECOL ENG*, *169*, 106328.
618 https://doi.org/10.1016/j.ecoleng.2021.106328
619 Blowes, D. W., Robertson, W. D., Ptacek, C. J., & Merkley, C. (1994). Removal of agricultural
620 nitrate from tile-drainage effluent water using in-line bioreactors. *Journal of contaminant*
621 *hydrology*, *15*(3), 207-221. https://doi.org/10.1016/0169-7722(94)90025-6
622 Cameron, S. G., & Schipper, L. A. (2010). Nitrate removal and hydraulic performance of organic
623 carbon for use in denitrification beds. *Ecological Engineering*, *36*(11), 1588-1595.
624 https://doi.org/10.1016/j.ecoleng.2010.03.010
625 Cawley, K. M. (2017). NEON User Guide to Dissolved gases in surface water
626 (DP1.20097.001) Version A. In: National Ecological Observatory Network.
627 Chapin, F. S., Matson, P. A., & Vitousek, P. M. (2011). Geology, Soils, and Sediments. In F. S.
628 Chapin, P. A. Matson, & P. M. Vitousek (Eds.), *Principles of Terrestrial Ecosystem*
629 *Ecology* (pp. 63-90). Springer New York. https://doi.org/10.1007/978-1-4419-9504-9_3
630 Christianson, L., Castello, A., Christianson, R., Helmers, M., & Bhandari, A. (2010).
631 HYDRAULIC PROPERTY DETERMINATION OF DENITRIFYING BIOREACTOR
632 FILL MEDIA. *Appl. Eng. Agric.*, *26*(5), 849-854.
633 Christianson, L. E., Bhandari, A., & Helmers, M. J. (2012). A Practice-oriented Review of
634 Woodchip Bioreactors for Subsurface Agricultural Drainage. *APPL ENG AGRIC*, *28*(6),
635 861-874. https://doi.org/10.13031/2013.42479
636 Christianson, L. E., Collick, A. S., Bryant, R. B., Rosen, T., Bock, E. M., Allen, A. L., . . .
637 Easton, Z. M. (2017). Enhanced Denitrification Bioreactors Hold Promise for Mid-
638 Atlantic Ditch Drainage. *Agricultural & environmental letters*, *2*(1), 1-5.
639 https://doi.org/10.2134/ael2017.09.0032
640 Christianson, L. E., Cooke, R. A., Hay, C. H., Helmers, M. J., Feyereisen, G. W., Ranaivoson, A.
641 Z., . . . Pluer, W. T. (2021). Effectiveness of denitrifying bioreactors on water pollutant
642 reduction from agricultural areas. *Transactions of the ASABE*, *64*(2), 641-658.
643 Christianson, L. E., Lepine, C., Sharrer, K. L., & Summerfelt, S. T. (2016). Denitrifying
644 bioreactor clogging potential during wastewater treatment. *Water Research*, *105*, 147-
645 156. https://doi.org/10.1016/j.watres.2016.08.067
646 Christianson, L. E., & Schipper, L. A. (2016). Moving Denitrifying Bioreactors beyond Proof of
647 Concept: Introduction to the Special Section. *J Environ Qual*, *45*(3), 757-761.
648 https://doi.org/10.2134/jeq2016.01.0013
649 Daigh, A. L. M., Zhou, X., Helmers, M. J., Pederson, C. H., Horton, R., Jarchow, M., &
650 Liebman, M. (2015). Subsurface Drainage Nitrate and Total Reactive Phosphorus Losses
651 in Bioenergy-Based Prairies and Corn Systems. *Journal of environmental quality*, *44*(5),
652 1638-1646. https://doi.org/10.2134/jeq2015.02.0080

David, M. B., Gentry, L. E., Cooke, R. A., & Herbstritt, S. M. (2016). Temperature and Substrate Control Woodchip Bioreactor Performance in Reducing Tile Nitrate Loads in East-Central Illinois. *Journal of environmental quality*, *45*(3), 822. https://doi.org/10.2134/jeq2015.06.0296

Davis, M. P., Martin, E. A., Moorman, T. B., Isenhart, T. M., & Soupir, M. L. (2019). Nitrous oxide and methane production from denitrifying woodchip bioreactors at three hydraulic residence times. *Journal of Environmental Management*, *242*, 290-297. https://doi.org/10.1016/j.jenvman.2019.04.055

Diaz, R. J., & Rosenberg, R. (2008). Spreading Dead Zones and Consequences for Marine Ecosystems. *SCIENCE*, *321*(5891), 926-929. https://doi.org/10.1126/science.1156401

Directive, E. U. Water Framework. (2000). Directive 2000/60/EC of the European Parliament. *Off J Eur Commun Legis L*, *327*(1), 1-71.

Dodge, R., Clemmens, A., & Replogle, J. (2001). Water measurement manual. *A Water Resources Technical Publication [Internet]. US Department of the Interior, Bureau of Reclamation*.

Díaz-García, C., Martínez-Sánchez, J. J., Maxwell, B. M., Franco, J. A., & Álvarez-Rogel, J. (2021). Woodchip bioreactors provide sustained denitrification of brine from groundwater desalination plants. *J Environ Manage*, *289*, 112521-112521. https://doi.org/10.1016/j.jenvman.2021.112521

Easton, Z. M., Bock, E., & Stephenson, K. (2019). Feasibility of Using Woodchip Bioreactors to Treat Legacy Nitrogen to Meet Chesapeake Bay Water Quality Goals. *Environ. Sci. Technol*, *53*(21), 12291-12299. https://doi.org/10.1021/acs.est.9b04919

European Union. (1991). Council Directive 91/676/EEC of 12 December 1991 concerning the protection of waters against pollution caused by nitrates from agricultural sources. *Off. J. Eur. Communities*, *375*, 1-8.

FAO. (2022). Climate Smart Agriculture Sourcebook: Climate-smart crop production. *Food and Agriculture Organization of the United Nations.* Retrieved 12 Dec 2022 from https://www.fao.org/climate-smart-agriculture-sourcebook/production-resources/module-b1-crops/b1-conclusions/en/

Fenton, O., Healy, M. G., Brennan, F. P., Thornton, S. F., Lanigan, G. J., & Ibrahim, T. G. (2016). Holistic Evaluation of Field-Scale Denitrifying Bioreactors as a Basis to Improve Environmental Sustainability. *J ENVIRON QUAL*, *45*(3), 788-795. https://doi.org/10.2134/jeq2015.10.0500

Ghane, E., Feyereisen, G. W., Rosen, C. J., & Tschirner, U. W. (2018). Carbon Quality of Four-Year-Old Woodchips in a Denitrification Bed Treating Agricultural Drainage Water. *Transactions of the ASABE*, *61*(3), 995-1000. https://doi.org/10.13031/trans.12642

Gilmour, C., Henry, E., & Mitchell, R. (1992). SULFATE STIMULATION OF MERCURY METHYLATION IN FRESH-WATER SEDIMENTS. *Environ. Sci. Technol.*, *26*(11), 2281-2287. https://doi.org/10.1021/es00035a029

Gilmour, C. C., Podar, M., Bullock, A. L., Graham, A. M., Brown, S. D., Somenahally, A. C., . . . Elias, D. A. (2013). Mercury methylation by novel microorganisms from new environments. *Environmental science & technology*, *47*(20), 11810-11820.

Greenan, C. M., Moorman, T. B., Parkin, T. B., Kaspar, T. C., & Jaynes, D. B. (2009). Denitrification in wood chip bioreactors at different water flows. *Journal of environmental quality*, *38*(4), 1664. https://doi.org/10.2134/jeq2008.0413

Healy, M. G., Barrett, M., Lanigan, G. J., João Serrenho, A., Ibrahim, T. G., Thornton, S. F., . . . Fenton, O. (2015). Optimizing nitrate removal and evaluating pollution swapping trade-offs from laboratory denitrification bioreactors. *Ecological Engineering*, *74*(C), 290-301. https://doi.org/10.1016/j.ecoleng.2014.10.005

Healy, M. G., Ibrahim, T. G., Lanigan, G. J., Serrenho, A. J., & Fenton, O. (2011). Nitrate removal rate, efficiency and pollution swapping potential of different organic carbon media in laboratory denitrification bioreactors. *Ecological Engineering*, *40*. https://doi.org/10.1016/j.ecoleng.2011.12.010

Hergoualc'h, K., Akiyama, H., Bernoux, M., Chirinda, N., Del Prado, A., Kasimir, Å., . . . Van Der Weerden, T. J. (2019). N2O emissions from managed soils, and CO2 emissions from lime and urea application. 2019 Refinement to the 2006 IPCC Guidelines for National Greenhouse Gas Inventories. *IPCC Intergovernmental Panel on Climate Change, Geneva*, 11-11.

Hoover, N., Bhandari, A., Soupir, M., & Moorman, T. (2016). Woodchip Denitrification Bioreactors: Impact of Temperature and Hydraulic Retention Time on Nitrate Removal. *J. Environ. Qual.*, *45*(3), 803-812. https://doi.org/10.2134/jeq2015.03.0161

Ikenberry, C. D., Soupir, M. L., Schilling, K. E., Jones, C. S., & Seeman, A. (2014). Nitrate-Nitrogen Export: Magnitude and Patterns from Drainage Districts to Downstream River Basins. *J ENVIRON QUAL*, *43*(6), 2024-2033. https://doi.org/10.2134/jeq2014.05.0242

Iowa Department of Agriculture and Land Stewardship, Iowa Department of Natural Resources and Iowa State University College of Agriculture and Life Sciences. (2017). Iowa Nutrient Reduction Strategy: A Science and Technology-Based Framework to Assess and Reduce Nutrients to Iowa Waters and the Gulf of Mexico.

Jia, A., & Yan, H. (2018). Visualized Analysis of Spatial Distribution of Dissolved Oxygen and Nitrogen Removal Efficiency in Constructed Wetland. In (pp. 781-789). Springer International Publishing. https://doi.org/10.1007/978-3-319-95588-9_65

Jéglot, A., Miranda-Velez, J. F., Plauborg, F., & Elsgaard, L. (2022). Nitrate removal and environmental side-effects controlled by hydraulic residence time in woodchip bioreactors treating cold agricultural drainage water. *Environmental Technology*, 1-10. https://doi.org/10.1080/09593330.2022.2091482

Khouni, I., Louhichi, G., & Ghrabi, A. (2021). Use of GIS based Inverse Distance Weighted interpolation to assess surface water quality: Case of Wadi El Bey, Tunisia. *Environmental Technology & Innovation*, *24*, 101892.

Knowles, R. (1982). Denitrification. *Microbiological reviews*, *46*(1), 43-70. https://doi.org/10.1128/mr.46.1.43-70.1982

Lawrence, N. C., Tenesaca, C. G., VanLoocke, A., & Hall, S. J. (2021). Nitrous oxide emissions from agricultural soils challenge climate sustainability in the US Corn Belt. *Proceedings of the National Academy of Sciences - PNAS*, *118*(46). https://doi.org/10.1073/pnas.2112108118j1of8

Manca, F., De Rosa, D., Reading, L. P., Rowlings, D. W., Scheer, C., Layden, I., . . . Grace, P. R. (2020). Nitrate removal and greenhouse gas production of woodchip denitrification walls under a humid subtropical climate. *Ecological engineering*, *156*, 105988. https://doi.org/10.1016/j.ecoleng.2020.105988

Manca, F., De Rosa, D., Reading, L. P., Rowlings, D. W., Scheer, C., Schipper, L. A., & Grace, P. R. (2021). Effect of soil cap and nitrate inflow on nitrous oxide emissions from

743 woodchip bioreactors. *ECOL ENG*, *166*, 106235.
744 https://doi.org/10.1016/j.ecoleng.2021.106235
745 Martin, E. A., Davis, M. P., Moorman, T. B., Isenhart, T. M., & Soupir, M. L. (2019). Impact of
746 hydraulic residence time on nitrate removal in pilot-scale woodchip bioreactors. *Journal*
747 *of Environmental Management*, *237*, 424-432.
748 https://doi.org/10.1016/j.jenvman.2019.01.025
749 Marvin-DiPasquale, M., Lutz, M. A., Brigham, M. E., Krabbenhoft, D. P., Aiken, G. R., Orem,
750 W. H., & Hall, B. D. (2009). Mercury Cycling in Stream Ecosystems. 2. Benthic
751 Methylmercury Production and Bed Sediment−Pore Water Partitioning. *Environmental*
752 *science & technology*, *43*(8), 2726-2732. https://doi.org/10.1021/es802698v
753 Maxwell, B. M., Birgand, F., Schipper, L. A., Christianson, L. E., Tian, S., Helmers, M. J., . . .
754 Youssef, M. A. (2019). Drying–Rewetting Cycles Affect Nitrate Removal Rates in
755 Woodchip Bioreactors. *J Environ Qual*, *48*(1), 93-101.
756 https://doi.org/10.2134/jeq2018.05.0199
757 Mississippi River/ Gulf of Mexico Task Force. (2020). *Hypoxia Task Force Nutrient Reduction*
758 *Strategies*. Retrieved 15 Jul 2021 from https://www.epa.gov/ms-htf/hypoxia-task-force-
759 nutrient-reduction-strategies
760 Mississippi River/Gulf of Mexico Watershed Nutrient Task Force. (2008). Gulf Hypoxia Action
761 Plan 2008 for reducing, mitigating, and controlling hypoxia in the Northern Gulf of
762 Mexico and improving water quality in the Mississippi River Basin. *Mississippi*
763 *River/Gulf of Mexico Watershed Nutrient Task Force*.
764 Moorman, T. B., Parkin, T. B., Kaspar, T. C., & Jaynes, D. B. (2010). Denitrification activity,
765 wood loss, and N.sub.2O emissions over 9 years from a wood chip bioreactor. *Ecological*
766 *Engineering*, *36*(11), 1567. https://doi.org/10.1016/j.ecoleng.2010.03.012
767 Myhre, G., Shindell, D., Breon, F. M., Collins, W., Fuglestvedt, J., Huang, J. P., . . . Young, P.
768 (2014). Anthropogenic and Natural Radiative Forcing. In T. F. Stocker, D. Qin, G. K.
769 Plattner, M. M. B. Tignor, S. K. Allen, J. Boschung, A. Nauels, Y. Xia, V. Bex, & P. M.
770 Midgley (Eds.), *Climate Change 2013: the Physical Science Basis* (pp. 659-740).
771 Cambridge Univ Press.
772 NRCS, USDA. (2015). Conservation Practice Standard Denitrifying Bioreactor Code 605.
773 *United States Department of Agriculture Natural Resources Conservation Service,*
774 *Washington, DC*.
775 NRCS, USDA. (2020). CONSERVATION PRACTICE STANDARD DENITRIFYING
776 BIOREACTOR CODE 605. *United States Department of Agriculture Natural Resources*
777 *Conservation Service, Washington D.C.*
778 Pebesma, E., Graeler, B., & Pebesma, M. E. (2015). Package 'gstat'. *Comprehensive R Archive*
779 *Network (CRAN)*, 1-0.
780 Pebesma, E., Racine, E., Fantini, A., & Blodgett, D. (2020). Package 'stars'. *Comprehensive R*
781 *Archive Network (CRAN)*.
782 Pedersen, T. L. (2020) patchwork: The Composer of Plots. R package version 1.1. 1. 2020. In.
783 Pester, M., Knorr, K.-H., Friedrich, M. W., Wagner, M., & Loy, A. (2012). Sulfate-reducing
784 microorganisms in wetlands - fameless actors in carbon cycling and climate change.
785 *Frontiers in microbiology*, *3*, 72. https://doi.org/10.3389/fmicb.2012.00072
786 Pulkkinen, J. T., Ronkanen, A.-K., Pasanen, A., Kiani, S., Kiuru, T., Koskela, J., . . . Vielma, J.
787 (2021). Start-up of a "zero-discharge" recirculating aquaculture system using woodchip

denitrification, constructed wetland, and sand infiltration. *Aquacultural Engineering*, *93*, 102161. https://doi.org/https://doi.org/10.1016/j.aquaeng.2021.102161

Reay, D. S., Smith, K. A., & Edwards, A. C. (2003). Nitrous oxide emission from agricultural drainage waters. *Global change biology*, *9*(2), 195-203. https://doi.org/10.1046/j.1365-2486.2003.00584.x

Rivas, A., Barkle, G., Stenger, R., Moorhead, B., & Clague, J. (2020). Nitrate removal and secondary effects of a woodchip bioreactor for the treatment of subsurface drainage with dynamic flows under pastoral agriculture. *Ecological engineering*, *148*, 105786. https://doi.org/10.1016/j.ecoleng.2020.105786

Sams, C. E. (2007). Methylmercury contamination: impacts on aquatic systems and terrestrial species, and insights for abatement. *Advancing the Fundamental Sciences*, 438-448.

Schaefer, A., Werning, K., Hoover, N., Tschirner, U., Feyereisen, G., Moorman, T. B., . . . Soupir, M. L. (2021). Impact of flow on woodchip properties and subsidence in denitrifying bioreactors. *Agrosystems, geosciences & environment*, *4*(1), n/a. https://doi.org/10.1002/agg2.20149

Schilling, K. E., Jones, C. S., Seeman, A., Bader, E., & Filipiak, J. (2012). Nitrate-nitrogen patterns in engineered catchments in the upper Mississippi River basin. *Ecological engineering*, *42*, 1-9.

Schipper, L. A., Cameron, S. C., & Warneke, S. (2010). Nitrate removal from three different effluents using large-scale denitrification beds. In (Vol. 36, pp. 1552-1557): Ecological Engineering.

Schmidt, C. A., & Clark, M. W. (2012). Evaluation of a Denitrification Wall to Reduce Surface Water Nitrogen Loads. *Journal of environmental quality*, *41*(3), 724-731. https://doi.org/10.2134/jeq2011.0331

Serrano, L. d. O., Borges, A. C., Pruski, F. F., & de Melo, M. C. (2020). A New Approach to Use Load Duration Curves to Evaluate Water Quality: A Study in the Doce River Basin, Brazil. *Water*, *12*(3), 811. https://doi.org/10.3390/w12030811

Shih, R., Robertson, W. D., Schiff, S. L., & Rudolph, D. L. (2011). Nitrate controls methyl mercury production in a streambed bioreactor. *Journal of environmental quality*, *40*(5), 1586. https://doi.org/10.2134/jeq2011.0072

Tchobanoglous, G., Burton, F. L., & Stensel, H. D. (2003). Wastewater Engineering: Treatment and Reuse .(Metcalf and Eddy Inc./McGraw-Hill, Inc, New York, USA). In: for Environmental Research Information Cincinnati.

Team, R. Core. R: a language and environment for statistical computing. Vienna, Austria: R Foundation for Statistical Computing. https://www. R-project. org.

US E. P. A. (2007). An approach for using load duration curves in the development of TMDLs. *Washington: Environmental Protection Agency*.

Voroney, R. P., & Heck, R. J. (2015). Chapter 2 - The Soil Habitat. In E. A. Paul (Ed.), *Soil Microbiology, Ecology and Biochemistry (Fourth Edition)* (pp. 15-39). Academic Press. https://doi.org/https://doi.org/10.1016/B978-0-12-415955-6.00002-5

Warneke, S., Schipper, L. A., Bruesewitz, D. A., McDonald, I., & Cameron, S. (2011). Rates, controls and potential adverse effects of nitrate removal in a denitrification bed. *Ecological Engineering*, *37*(3), 511-522. https://doi.org/10.1016/j.ecoleng.2010.12.006

White, S. A., Morris, S. A., Wadnerkar, P. D., Woodrow, R. L., Tucker, J. P., Holloway, C. J., . . . Santos, I. R. (2022). Anthropogenic nitrate attenuation versus nitrous oxide release from

a woodchip bioreactor. *Environmental pollution (1987)*, *300*, 118814-118814. https://doi.org/10.1016/j.envpol.2022.118814

Wickham, H., & Wickham, M. H. (2019). Package 'tidyverse'. *See http://tidyverse. tidyverse. org*, 1-5.